雪の圧縮特性の熱力学的検討(英文)

著者	桜田 良治, 栗山 弘
雑誌名	国立防災科学技術センター 研究報告
巻	26
ページ	89-103
発行年	1981-11
URL	http://doi.org/10.24732/nied.00000852

Report of the National Research Center for Disaster Prevention, No. 26, November 1981

551.322 : 536.7

A Thermodynamical Study on Compression Properties of Snow

By

Ryoji Sakurada

Master Course Student, The Technological University of Nagaoka,
Nagaoka, Niigata-Ken 949-54, Japan

And

Hiroshi Kuriyama

Institute of Snow and Ice Studies,
National Research Center for Disaster Prevention,
Nagaoka, Niigata-Ken, 940, Japan

Abstract

This is the report of a thermodynamical and experimental study on the compression characteristics of snow. Theoretically, the strains of void air and pore water in the compacted snow decrease the elasticity and viscosity of ice particles. The experiment gives a result that the mechanical property of snow varies from plasticity to elasticity. And theory also indicates that the exclusion of void air or pore water with compression lessens its strain effect and brings on the above result.

Nomenclatures

I_s = interacting force,
ρ_s = bulk density of the ice phase,
ρ_g = bulk density of the gas phase,
ρ_t = $\rho_s + \rho_g$ (for the infinitesmal volume),
e_s, e_g = internal energy of the ice phase and the gas phase,
e_t = total internal energy,
σ_{ij}, P_{ij} = stress tensors of the ice phase and the gas phase,
u_i, v_i = displacement components of the ice phase and the gas phase,
ϵ_{ij}, ε_{ij} = symmetric tensors of strain of the ice phase and the gas phase,
$\dot{\epsilon}_{ij}$, $\dot{\varepsilon}_{ij}$ = symmetric tensors of strain velocity of the ice phase and the gas phase,
J_i^{sf}, J_i^{gf} = heat generated by friction among themselves, ice particles and gas,

J_i^{sw}, J_i^{gw} = heat generated by friction between ice particles and the side of mold, or gas and the side of mold,

J_i^{sv}, J_i^{gv} = heat dispersed by vibration of compacted snow,

J_i^{tf} = total heat generated by friction among themselves, ice particles and gas ($= J_i^{sf} + J_i^{gf}$),

J_i^{tw} = total heat generated by friction between ice particles and the side of mold, or between gas and the side of mold ($= J_i^{sw} + J_i^{gw}$),

J_i^{tv} = total heat dispersed by vibration of compacted snow ($= J_i^{sv} + J_i^{gv}$),

T = temperature (°K),

S_f = entropy flow,

S_p = entropy production,

S_t = total entropy,

σ_{dij} = deviator component of stress tensor of ice phase,

ϵ_{dij} = deviator component of strain tensor of ice phase,

P_{dij} = deviator component of stress tensor of gas phase,

ε_{dij} = deviator component of strain tensor of gas phase,

$\eta_g, \eta_g', \eta_w, \eta_i, \eta_i'$ (i = 1, 2, 4) = viscous constants,

$\nu_g, \nu_w, \nu_i, \nu_i'$ (i = 1, 2, 4) = elastic constants,

Z^* = complex impedance,

j = unit of imaginary number ($\sqrt{-1}$),

ω = angular frequency,

M = mass of ice particles,

σ, ε = stress and strain of snow (kgf/cm^2 and %),

E_c = initial compaction energy (kgf · cm/cm^3),

W_r = weight of rammer (kgf),

H = dropping height of rammer (cm),

N_b = compaction times per layer,

N_l = number of layers,

V_m = volume of mold (cm^3),

ρ = density of snow (g/cm^3),

e = void ratio,

G_s = specific gravity of ice,

A = cross-sectional area of sample (cm^2),

h_n = sample height at n-th load step (cm),

W_n = wet weight of sample at n-th load step (gf),

w_n = water content of snow (%),

γ_w = weight of water per unit volume (gf/cm^3),

h_s = value which is obtained by dividing the whole volume of sample by its cross-sectional area (cm),

C_c = compression index,

e_1, e_2 = two void ratios of straight part on $e - \mathrm{Log}_{10}\,\sigma$ curve,

σ_1, σ_2 = stresses corresponding to e_1 and e_2 respectively (kgf/cm^2),

η = coefficient of viscosity (kgf · sec/cm^2),
P = load (kgf),
D_0 = diameter of sample (cm),
V = rate of loading (cm/sec),
E_r = relaxation modulus (kgf/cm^2),
E_i = initial Young modulus (kgf/cm^2),
J_t = compliance (cm^2/kgf),
$E_{r\,min}$ = minimum value of E_r (kgf/cm^2),
$J_{t\,max}$ = maximum value of J_t (cm^2/kgf),
η_{cr} = limiting coefficient of viscosity, corresponding to the minimum point of E_r or the maximum point of J_t (kgf · sec/cm^2),
n = porosity (%),
subscript rev = reversible component, and
subscript irr = irreversible component.

1. Introduction

When snow is artificially compressed, such phenomena as rearrangement and crushing of ice particles, reduction of void ratio, exclusions of void air and pore water, etc. occur. These factors, which are difficult to measure, play important roles in compaction properties of snow. Load-displacement relationship and stress-strain relationship alone are insufficient to investigate the dynamical behavior of compacted snow.

The authors attempt to apply irreversible thermodynamics to the analysis of the above behavior. And this approach may yield the qualitative interpretation of compaction properties of snow that the strains of void air and pore water decrease the elasticity and the viscosity of ice particles. The effect of void air is also recognized in the results of the experiment in which load-displacement relationships are obtained from pre-compacted snow with various values of energy.

2. Experimental procedures and equipments

The compression characteristics of snow are affected by many factors: nature of snow, water content, initial compaction energy, rate of loading, temperature of snow, etc. In the present experiment, only the initial compaction energy is varied for five cases and the other factors are kept unchanged, considering the complexity of the effect of each factor. Experimental conditions are shown in Table 1. Fig. 1 illustrates the general outline of the equipment for the experiment, and Photo 1 shows the general view of the

Table 1 Experimental Conditions

No.	Items	Conditions
1	Nature of snow	New powder snow
2	Water content of snow	0%
3	Initial compaction energy	0.066, 0.100, 0.199, 0.399, 126.7 (kgf · cm/cm^3)
4	Rate of loading	6.1 (%/min.)
5	Temperature of snow	−5.0°C

equipment. Experimental procedures are following. First, samples of new-powder snow, with 0% of water content, which order was attained by keeping the snow sample in a room at $-5^{\circ}C$ for serveral hours, are pre-compacted under five grades of compaction energy. Then they are packed into molds of 100 mm in diameter and 170 mm in height. Under the lateral confinement, the snow sample is compacted until its compressive strain amounts to 47%, which is the limit of the piston stroke. Load and displacement are measured with the load cell and the displacement transducer, and are registered on a X-Y recorder. Photo 2 shows the compacted snow in the mold.

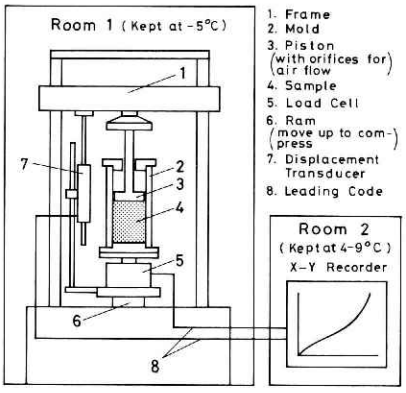

Fig. 1 Snow compression test equipments.

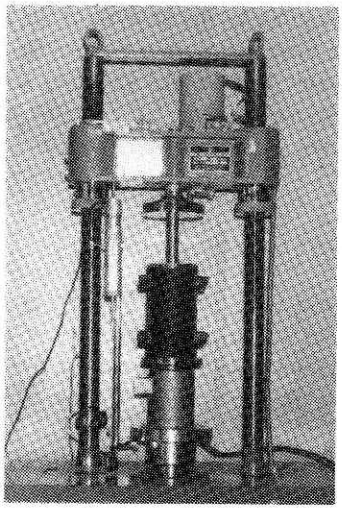

Photo. 1 Snow compression test equipment.

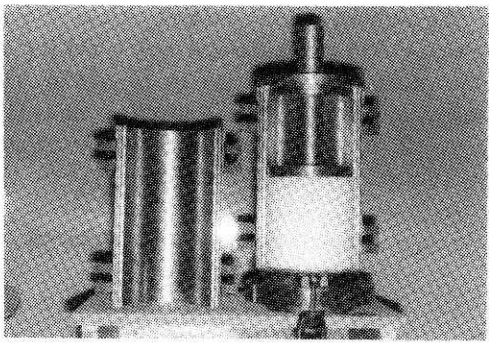

Photo. 2 Compacted snow in the Mold.

3. Viscoelastic properties of snow

Snow is a typical material showing viscoelastic characteristics. The fundamental investigations of the viscoelastic characteristics of snow have been early reported by Yoshi-

da (1953) and Kojima (1954). Kinoshita (1957) has described the snow cover as consisting of a parallel connection of different Maxwell elements.

In Fig. 2 the variation in compression properties of snow is shown by using the dynamical models and the electric circuit models, in which the internal resistances of void air and pore water (hidden coordinates) are represented as Maxwell elements according to the rock mechanics (The Japan Society of Civil Engineers, 1975). The exclusion of hidden coordinates with compression brings the elimination of excess Maxwell elements.

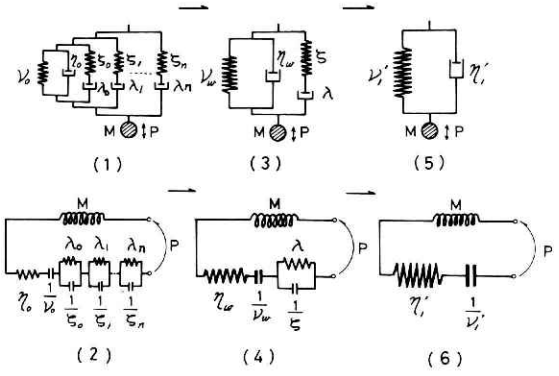

Fig. 2 Viscoelastic and electric circuit models of snow compression.

It is known that the Voigt model corresponds to a series connection of electric circuits, and the Maxwell model to a parallel connection (Nakagawa and Kanbe, 1970). For Fig. 2 complex impedances of the electric circuit models are given as follows:

for Fig. 2(2)

$$Z^* = j\omega M + \eta_o + \frac{\nu_o}{j\omega} + \frac{1}{\frac{1}{\lambda_o} + \frac{1}{\zeta_o / j\omega}} + \frac{1}{\frac{1}{\lambda_1} + \frac{1}{\zeta_1 / j\omega}} + \cdots + \frac{1}{\frac{1}{\lambda_n} + \frac{1}{\zeta_n / j\omega}} \quad (1)$$

for Fig. 2(4)

$$Z^* = j\omega M + \eta_w + \frac{\nu_w}{j\omega} + \frac{1}{\frac{1}{\lambda} + \frac{1}{\zeta / j\omega}} \quad (2)$$

for Fig. 2(6)

$$Z^* = j\omega M + \eta_1 + \frac{\nu_1}{j\omega} \quad (3)$$

4. Analysis of the effect of void air or pore water

4.1 Energy equations and entropy equations

Irreversible thermodynamics has been applied to the fields of soil and rock mechanics. For example, in rock mechanics (The Japan Society of Civil Engineers, 1975) the influ-

ences of the strain components of pore water on the viscoelastic properties of rock frames are discussed. And in soil mechanics Ishihara (1965) theoretically explained the consolidation of a porous material with heat effect. In this study, a similar analysis is made to attempt as to the effect of void air or pore water in the compacted snow. The following assumptions are made for simplification in developing the theory:

1. Compacted snow consists of ice particles and voids which are distributed uniformly over its volume.
2. Voids are filled with either air or water.
3. Both void air and pore water are compressible.
4. Compacted snow constitutes a two-phase system: ice-gas system or ice-water system (see Fig. 3).

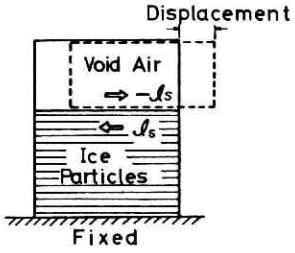

Fig. 3 Simplified configuration of Ice-Gas system.

The energy equations for each phase and entropy equations from Gibbs's principle of gas are shown below. The equations are derived according to Ref. 1, 8. The notations used in this paper are shown in Nomenclatures.

Energy equations:

for ice phase

$$\rho_s \frac{de_s}{dt} = \sigma_{ij}\dot{\varepsilon}_{ij} - \left(J_i^{sf} + J_i^{sw} + J_i^{sv} \right)_{,i} + I_s \left(\dot{v}_i - \dot{u}_i \right) - I_s \dot{u}_i \tag{4}$$

for gas phase

$$\rho_g \frac{de_g}{dt} = P_{ij}\dot{\varepsilon}_{ij} - \left(J_i^{gf} + J_i^{gw} + J_i^{gv} \right)_{,i} + I_s \dot{u}_i \tag{5}$$

for total system

$$\rho_t \frac{de_t}{dt} = \rho_s \frac{de_s}{dt} + \rho_g \frac{de_g}{dt} = \sigma_{ij}\dot{\varepsilon}_{ij} + P_{ij}\dot{\varepsilon}_{ij} - \left(J_i^{tf} + J_i^{tw} + J_i^{tv} \right)_{,i} + I_s \left(\dot{v}_i - \dot{u}_i \right) \tag{6}$$

Entropy equations:

$$\rho_t \frac{ds_t}{dt} = \underbrace{-\left\{ \left(\frac{J_i^a}{T} \right)_{,i}^{tf} + \left(\frac{J_i^b}{T} \right)_{,i}^{tw} + \left(\frac{J_i^c}{T} \right)_{,i}^{tv} \right\}}_{\rho_t \frac{ds_f}{dt}}$$

$$+ \underbrace{\frac{I}{T}\left(\sigma_{ij}^{irr}\dot{\varepsilon}_{ij} + P_{ij}^{irr}\dot{\varepsilon}_{ij} \right) + \frac{I_s}{T}\left(\dot{v}_i - \dot{u}_i \right) - \left\{ J_i^{tf}\frac{T_{,i}}{T^2} + J_i^{tw}\frac{T_{,i}}{T^2} + J_i^{tv}\frac{T_{,i}}{T^2} \right\}}_{\rho_t \frac{ds_p}{dt}} \tag{7}$$

Alternatively,

$$\rho_t \frac{ds_t}{dt} = \underbrace{-\left\{\left(\frac{J_i^a}{T}\right)_{,i}^{tf} + \left(\frac{J_i^b}{T}\right)_{,i}^{tw} + \left(\frac{J_i^c}{T}\right)_{,i}^{tv}\right\}}_{\rho_t \frac{ds_f}{dt}} + \underbrace{\frac{I}{T}\left(\sigma_{ij}\dot{\epsilon}_{ij}^{irr} + P_{ij}\dot{\varepsilon}_{ij}^{irr}\right) + \frac{I_s}{T}\left(\dot{v}_i - \dot{u}_i\right) - \left\{J_i^{tf}\frac{T_{,i}}{T^2} + J_i^{tw}\frac{T_{,i}}{T^2} + J_i^{tv}\frac{T_{,i}}{T^2}\right\}}_{\rho_t \frac{ds_p}{dt}} \quad (8)$$

4.2 Strain effect of void air

The entropy production terms on the right side of Eq. (7) are :

$$\rho_t T\frac{ds_p}{dt} = \sigma_{ij}^{irr}\dot{\epsilon}_{ij} + P_{ij}^{irr}\dot{\varepsilon}_{ij} + \left\{I_s\left(\dot{v}_i - \dot{u}_i\right) - \left(J_i^{tf}\frac{T_{,i}}{T} + J_i^{tw}\frac{T_{,i}}{T} + J_i^{tv}\frac{T_{,i}}{T}\right)\right\} \quad (9)$$

In Eq. (9) we attempt to analyze only the 1st and 2nd terms, because the compacted snow in the present experiment has no influence of heat flux and suction force. And the following assumptions are introduced:

1. There exists no relative displacement between the ice phase and the gas phase, and
2. Void air has the same rigid displacement as the ice particle, but makes a deformation different from it.

And the authors assume a linear relationship between σ_{dij}^{rev} (the reversible compoennt of σ_{dij}), the deviator component of strain tensor of ice phase ϵ_{dij} and the deviator component ot strain tensor of gas phase ε_{dij}, whose coefficients are $2\nu_1$ and $2\nu_2$, respectively.

A similar relationship is supposed for P_{dij}^{rev} (the reversible component of P_{dij} which is the deviator component of stress tensor of gas phase), ϵ_{dij} and ε_{dij} which have $2\nu_2$ and $2\nu_4$, respectively, as proportional constants.

For σ_{dij}^{irr} (the irreversible component of σ_{dij}), $\dot{\epsilon}_{dij}$ and $\dot{\varepsilon}_{dij}$ (" $\cdot$ " represents the time derivative) and for P_{dij}^{irr} (the irreversible component of P_{dij}), $\dot{\epsilon}_{dij}$ and $\dot{\varepsilon}_{dij}$, linear relations which have the proportional constants $2\eta_1$, $2\eta_2$ and $2\eta_4$, respectively, are also presumed. η_1 , η_2 and η_4 , are the viscous contants.

Then, for the stress-stain relationship of ice particles, Eqs. (10) and (11) which include the effect of void air (η_2) can be obtained. Derivations of Eqs. (10), (11) are made according to Ref. 1, 8.

$$\sigma_{dij} = 2\nu_g\epsilon_{dij} + 2\eta_g D\epsilon_{dij} \quad (10)$$

$$\nu_g = \frac{\nu_1\eta_4}{\eta_4}, \quad \eta_g = \frac{\eta_1\eta_4 - \eta_2^2}{\eta_4} \qquad \left(D = \frac{d}{dt}\right) \quad (11)$$

If the strain of void air has no influence ($\eta_2 = 0$), Eqs. (10) and (11) are reduced to Eqs. (12) and (13).

$$\sigma_{dij} = 2\nu_g\epsilon_{dij} + 2\eta_g^1 D\epsilon_{dij} \quad (12)$$

$$\nu_g = \frac{\nu_1 \eta_4}{\eta_4} \quad , \quad \eta_g^1 = \frac{\eta_1 \eta_4}{\eta_4} \tag{13}$$

Eqs. (11) and (13) and the condition $\frac{d s_p}{d t} \geq 0$ (see Eq. (9)) provide the following relations:

$$\nu_g = \nu_g \quad , \quad \eta_g^1 > \eta_g \tag{14}$$

Relations (14) yeild three results as to the strain of void air:

1. The strain of void air exerts no or slight influence on the elasticity of ice particles.
2. It decreases the viscosity of ice particles.
3. As void air is removed by compression, the above effect decreases. Consequently, compacted snow comes to show the characteristics of a hard viscoelastic body.

Eqs. (10) and (12) are expressed as a series connection of electric circuits (see Fig. 4) and their complex impedances are as below:

$$Z^* = j\omega M + \eta_g + \frac{\nu_g}{j\omega} \tag{15}$$

$$Z^* = j\omega M + \eta_g^1 + \frac{\nu_g}{j\omega} \tag{16}$$

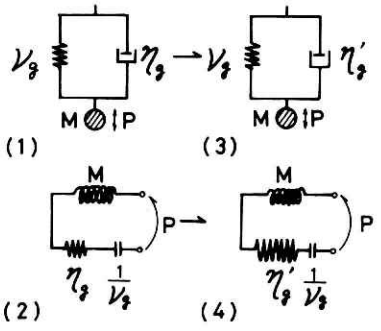

Fig. 4 Viscoelastic and electric circuit models of snow compression in case of considering void air.

4.3 Strain effect of pore water

In this article, the wet snow as seen in Hokuriku district is considered. The stress-strain relationship of the ice-water system is discussed in the similar way as in Article 4.2.

The void air is replaced with pore water; then Eqs. (17) and (18) are obtained.

Viscous and elastic constants of pore water are represented as η_i' and ν_i' ($i = 1, 2, 4$), respectively, which are defined in a way similar to η_i and ν_i of void air.

$$\sigma_{dij} = 2\nu_w \epsilon_{dij} + 2\eta_w D\epsilon_{dij} + 2\frac{\zeta D}{D + \zeta/\lambda}\epsilon_{dij} \tag{17}$$

$$\left.\begin{aligned} \nu_w &= \frac{\nu_1' \nu_4' - \nu_2'^2}{\nu_4'} \quad , \quad \eta_w = \frac{\eta_1' \eta_4' - \eta_2'^2}{\eta_4'} \\ \zeta &= \frac{(\nu_2' \eta_4' - \eta_2' \nu_4')^2}{\nu_4' \eta_4'^2} \quad , \quad \lambda = \frac{(\nu_2' \eta_4' - \eta_2' \nu_4')^2}{\nu_4'^2 \eta_4'} \end{aligned}\right\} \tag{18}$$

When pore water has no influence ($\nu_2' = \eta_2' = 0$), it follows that:

$$\sigma_{dij} = 2\nu_1' \epsilon_{dij} + 2\eta_1' D\epsilon_{dij} \tag{19}$$

From Eq. (18) and the condition $\frac{d s_p}{d t} \geq 0$, the relations as below are derived:

$$\nu_1' > \nu_w \quad , \quad \eta_1' > \eta_w \tag{20}$$

According to the relations (20), the strain of pore water decreases the elasticity and viscosity of ice particles. Therefore, exclusion of pore water with compression makes a recovery of the elasticity and viscosity which is equivalent to the removal of excess Maxwell elements.

Equations (17) and (19) are shown as viscoelastic and electric circuit models in Figs. 2(3), 2(4) and 2(5), 2(6) and the complex impedances are equivalent to Eqs. (2) and (3).

5. Comparison of theoretical and experimental studies

5.1 Compaction energy versus stress-strain relation

Variation of stress σ – strain ε relationship with different initial compaction energy E_c is illustrated in Fig. 5. The σ – ε relationship for each value of E_c is represented as a curved line whose gradient becomes larger with increasing E_c. In other words, this tendency is maintained to be attributable to the initial differences in the void ratio and the arrangement of ice particles. In Fig. 5, samples No. 1–No. 4 are artificially compacted ones (see Table 1) and No. 5 naturally compacted one sampled from a road.

Herein the compaction energy of Proctor (1933) is given as follows:

$$E_c = \frac{1}{V_m}(W_r \cdot H \cdot N_b \cdot N_l) \tag{21}$$

To estimate E_c of the road sample, the relationship between the initial compaction energy E_c and the density of snow ρ is obtained in the following form (Fig. 6):

$$E_c = 6460\rho^{7.500} \tag{22}$$

From Eq. (22) E_c of the road sample ($\rho = 0.592$ (g /cm^3)) is calculated at 126.7 (kgf·cm/cm^3).

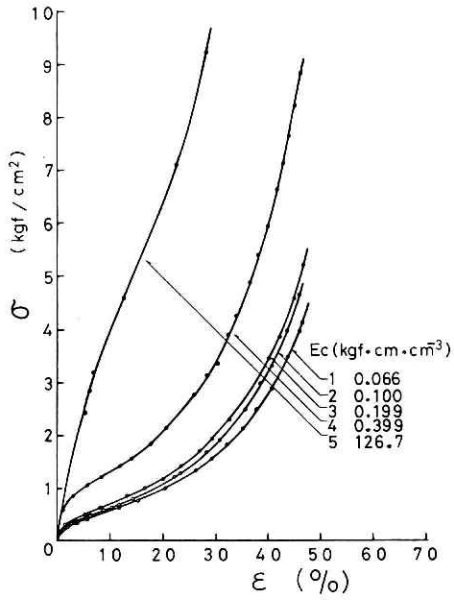

Fig. 5 Variation of stress σ-strain ε relationship with different values of initial compaction energy Ec.

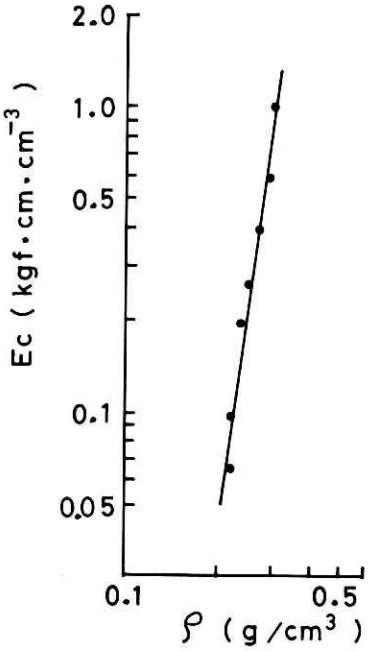

Fig. 6 Initial compaction energy Ec versus initial density of snow ρ.

5.2 Compressibility of snow

Figure 7 shows the relationship between void ratio e and $\log_{10}\sigma$. e is given as below (Kawakami, 1974):

$$e = \frac{\gamma_w \cdot G_s \cdot A \cdot h_n (1 + w_n/100)}{W_n} - 1 = \frac{h_n}{h_s} - 1 \qquad (23)$$

$$h_s = \frac{W_h}{\gamma_w \cdot G_s \cdot A (1 + w_n/100)}$$

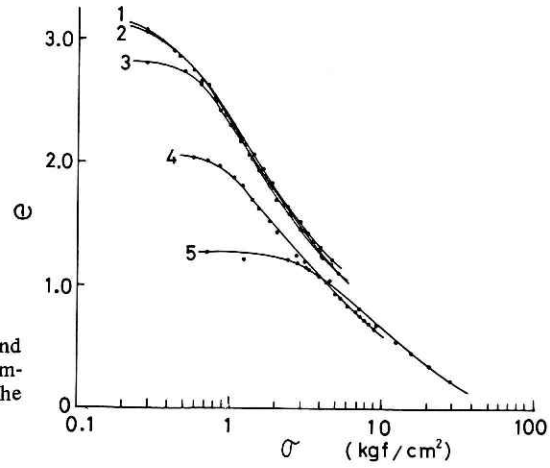

Fig. 7 Relationship between void ratio e and stress σ for different values of initial compaction energy Ec. The numbers of the curves correspond to those in Fig. 5.

The gradient of the straight part of $e - \log_{10}\sigma$ curve is called "compression index" C_c . This denotes the degree of compression of a sample and is given as follows:

$$C_c = \frac{\Delta e}{\log_{10} \Delta\sigma} = \frac{e_1 - e_2}{\log_{10} \frac{\sigma_1}{\sigma_2}} \tag{24}$$

Table 2 Calculated compression index C_c for each initial compaction energy E_c

No.	E_c(kgf·cm/cm³)	C_c
1	0.066	1.825
2	0.100	1.823
3	0.199	1.782
4	0.399	1.367
5	126.7	1.054

The value of C_c for each value of E_c is calculated to get the result shown in Table 2. The values in Table 2 indicate a tendency that the compressibility of snow is higher when snow is initially more loosely compacted.

5.3 Change in mechanical property of compacted snow

Figure 8 shows the relationship between stress σ and "relaxation modulus" E_r which is defined as σ/ε. In this figure, E_r first decreases to the minimum value $E_{r\,min}$ with the increment of σ and then augments again. Each $\sigma - E_r$ curve has an extreme point; this is similar to a property of viscoelastic materials (Jastrzebski, 1959).

Table 3 gives the initial Young modulus E_i. This is the value of E_r at the intersection point where the prolongation of the linear part of $E_r - \sigma$ relationship crosses the abscissa. It is recognized in Table 3 that E_i has a larger value when the initial compaction energy is larger.

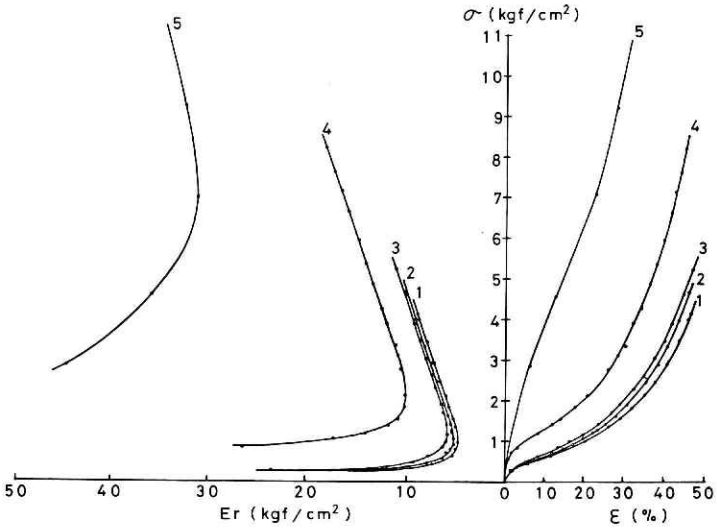

Fig. 8 Relationship between stress σ and relaxation modulus Er in comparison with stress σ-strain ε relationship.

Table 3 Initial Young Modulus E_i

No.	E_c (kgf·cm/cm³)	E_i (kgf/cm²)
1	0.066	3.2
2	0.100	3.5
3	0.199	3.9
4	0.399	6.5
5	126.7	18.6

Figure 9 illustrates the relationship between the coefficient of viscosity η and "relaxation modulus" E_r. Viscosity η is defined as follows:

$$\eta = \frac{P}{D_0 V} \tag{25}$$

With the increment of compression, η augments monotonously, and E_r first decreases to a minimum value and then augments again. The broken line in Fig. 9 passes through the minimum value $E_{r\min}$ for each experiment and is expressed in the form:

$$\eta_{cr} \cdot \frac{1}{E_{r\,\min}} = 10200 \tag{26}$$

Figure 10 represents the relation between η and "compliance" J_t which is a reciprocal of the relaxation modulus E_r. In contract with the behavior of E_r in Figs. 8 and 9, J_t first increases to a maximum value $J_{t\max}$ and decreases again. For the broken curve in Fig. 10, Eq. (27) can be obtained:

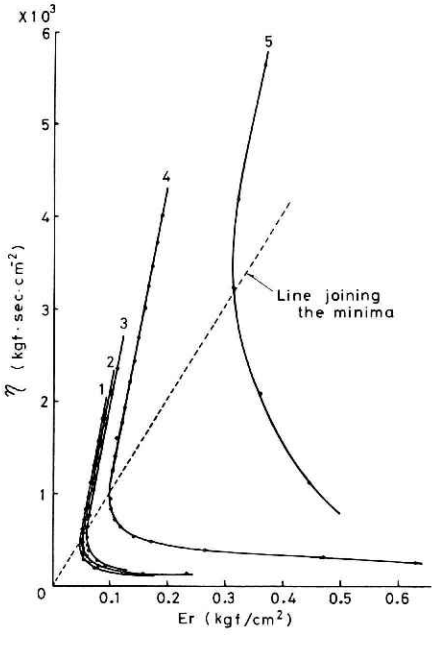

Fig. 9 Variation of coefficient of viscosity η with relaxation modulus Er.

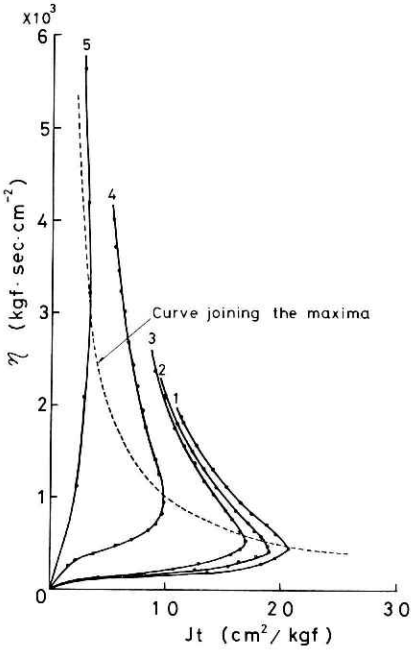

Fig. 10 Variation of coefficient of viscosity η with compliance Jt.

$$\eta_{cr} \cdot J_{t\max} = 10200 \tag{27}$$

Here the theoretical analysis made in Articles 4.2 and 4.3 is applied to the results of the experiment. Fig. 11 gives the relations of $\eta - E_r$, $\eta - J_t$ and $\eta - n$ of the sample No. 4 which is chosen as a representative and the electric circuit models previously shown in Fig. 2. The notation "n", which is defined as $e/(1+e)$, is called "porosity" (Kawakami, 1974). In this figure, two regions concerned in the theorogical property are obviously recognized: the plastic region and the elastic region. With the advance of compression, the mechanical characteristics change from plastic region to elastic.

Comparing this result with the electric models, the excess elements of the complex impedance Z^* are excluded by the reduction of void air or pore water (see relation $\eta - n$ in Fig. 11), and Z^* becomes simpler and to have a larger value with the increase in compression. In other words, the variation in electric circuit models corresponds to the increment of internal resistance of ice particles and to the reduction of strain effect of void air or pore water due to the exclusion of air or water with compression.

And the linear change of the compacted snow in the elastic region can be explained by the energy Eq. (6).

$$\rho_t \frac{de_t}{dt} = \rho_s \frac{de_s}{dt} + \rho_g \frac{de_g}{dt} = \sigma_{ij}\dot{\varepsilon}_{ij} + P_{ij}\dot{\varepsilon}_{ij} - (J_i^{tf} + J_i^{tw} + J_i^{tv})_{,i} + I_s(\dot{v}_i - \dot{u}_i) \tag{6}$$

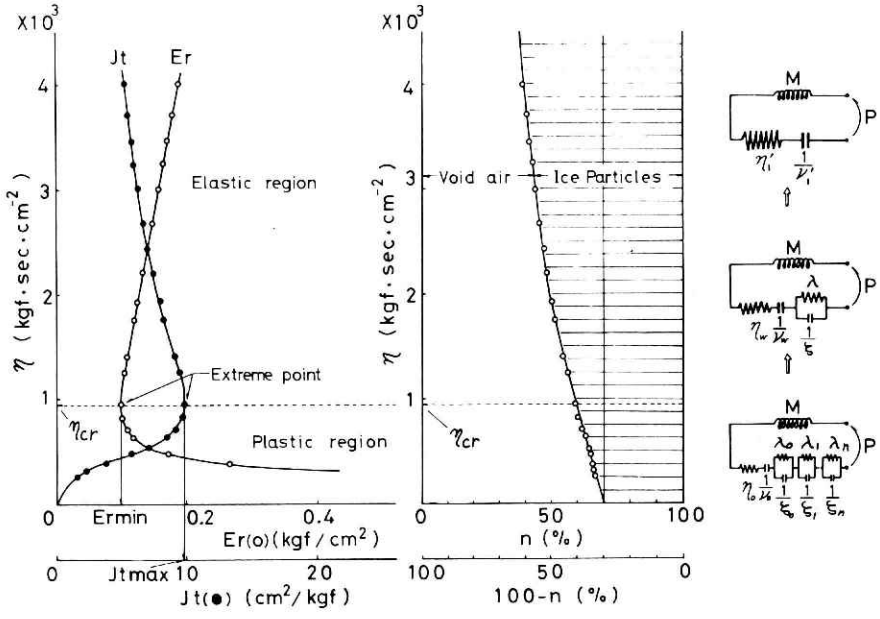

Fig. 11 Change in viscoelastic characteristics of compacted snow.

In the initial stage of compression, snow absorbs the dynamic energy of loading in the form of friction heat and behaves as plastic. In this stage, some heat is produced: the heat generated by friction among themselves, the ice particles, void air and pore water (J_i^{tf}) and the heat generated by friction between the ice particles and the sides of mold (J_i^{tw}).

In the elastic region, the bulk transformation of snow gradually decreases, and the dynamic energy is dispersed in the form of vibration energy (J_i^{tv}).

A study with respect to the accumulation and the dispersion of energy has been made in soil mechanics by Yamashita and Shirai (1981).

6. Conclusions

In this study, the authors experimentally observed the variation of compressive strength of snow in the mold, and analyzed the mechanism of its change by using the electric models based on irreversible thermodynamics. The following conclusions were obtained from this study.

1. Change in compaction properties of snow is clearly recognized: the $\eta - E_r$ and $\eta - J_t$ relationships have extreme values at which plasticity balances with elasticity.
2. The strain effect of void air and pore water decreases both the elasticity and viscosity of ice particles.
3. Exclusion of void air reduces the strain effect, and the compacted snow comes to show a hard viscoelastic property.
4. Transformation of the mechanical property from plastic region to elastic is equivalent to the removal of excess impedance elements and to the increase in complex impedance.
5. In the initial stage of compression, snow takes a plastic behavior and absorbs the dynamical energy of loading in the form of friction heat.
6. In the elastic region, snow shows elastic properties and disperses the dynamical energy to the mold in the form of vibration energy.

7. Acknowledgement

This study was conducted during the industrial training terms of The Technological University of Nagaoka from October 1979 to March 1980 at the Institute of Snow and Ice Studies, National Research Center for Disaster Prevention, Nagaoka.

The authors are grateful to Mr. I. Nohara, Head of the 3rd. Laboratory of the Institute, and to Mr. T. Kobayashi, a member of the Laboratory for their valuable advice and suggestion during the experiment, and to Mr. Y. Kawahara, Assistant of Civil Engineering, The Technological University of Nagaoka, for his generous review of the paper.

8. References

1) Ishihara, K. (1965): Theory of Consolidation of a Porous Material with Heat Effect based on the Irreversible Thermodynamics, Trans. of JSCE, **No. 113**, Jan.
2) Jastrzebski, D. (1959): Nature and Properties of Engineering Materials, John Wiley & Sons, Inc., pp. 156–171.
3) Kawakami, F. (1974): Newly-Published Soil Mechanics, Morikita Syuppan, pp. 50–74. (in Japanese)
4) Kinoshita, S. (1957): The Relation between the Deformation Velocity of Snow and Two Types of its Deformation (Plastic and Destructive.), Low Temperature Science, Ser. A, **16**. (in Japanese)
5) Kojima, K. (1954): Visco-Elastic Property of Snow, Low Temperature Science, Ser. A, **12**. (in Japanese)
6) Nakagawa, T. and Kanbe, H. (1970): Rheology, Misuzushobo, pp. 432–455. (in Japanese)

7) Proctor, R. R. (1933): Fundamental Principles of Soil Compaction, *Eng. News Record,* Aug. 31, Sept. 7, 21,28.
8) The Japan Society of Civil Engineers (1975): Rock Mechanics for Civil Engineers, Gihodo, pp. 204–215. (in Japanese)
9) Yamashita, T. and Shirai, K. (1981): Studies on the Heat Generation originated from Soil Compaction, The Japanese Society of Soil Mechanics and Foundation Engineering, **Vol. 29, No. 1**, pp. 57–63. (in Japanese)
10) Yoshida, Z. (1953): Visco-Elastic Property and Break-Down Resistance of Snow, Low Temperature Science, Ser. A, **10**. (in Japanese)

(Manuscript received June 27, 1981)

雪の圧縮特性の熱力学的検討

桜田良治*

長岡技術科学大学大学院
修士課程建設工学専攻

栗山　弘

国立防災科学技術センター
雪害実験研究所

雪は圧縮の進行につれて，塑性状態から弾性状態へと変化していくことが実験で確かめられた．また雪中の間隙空気および間隙水の歪みが氷粒子に及ぼす効果は熱力学により氷粒子の弾性と粘性を低下させることが判明した．一方，圧縮に伴う間隙空気，間戟水の排除は，この歪み効果を低下させること，つまり雪が次第に強粘弾性体の性質を帯びてくることを示唆している．

＊　昭和54年10月から3月まで，雪害実験研究所において，実務訓練を行なった．